Structures 38 (2022) 108–122

Contents lists available at ScienceDirect

Structures

journal homepage: www.elsevier.com/locate/structures

Calibration of the numerical model of a freight railway vehicle based on experimental modal parameters

D. Ribeiro [a,*], C. Bragança [b], C. Costa [c], P. Jorge [d], R. Silva [d], A. Arêde [d], R. Calçada [d]

[a] CONSTRUCT-LESE, School of Engineering, Polytechnic of Porto, Porto, Portugal
[b] Department of Structural Engineering, Federal University of Minas Gerais, Belo Horizonte, Brazil
[c] CONSTRUCT-LESE, Polytechnic Institute of Tomar, Tomar, Portugal
[d] CONSTRUCT-LESE, Faculty of Engineering, University of Porto, Porto, Portugal

ARTICLE INFO

Keywords:
Freight wagon
FE model
Dynamic tests
Model updating
Genetic algorithm

ABSTRACT

The simulation of the dynamic behavior of the train-track system is strongly dependent on the accuracy of the numerical models of the train and track subsystems. The use of calibrated numerical models of the railway vehicles, based on experimental data, enhances their ability to correctly reproduce the dynamic responses of the train under operational conditions. In this scope, studies involving the experimental calibration of freight wagon models are still scarce. This article aims to fill this gap by presenting an efficient methodology for the calibration of a numerical model of a freight railway wagon based on experimental modal parameters. A dynamic test was performed during the unloading operation of the train, adopting a dedicated approach which does not interfere with its tight operational schedule. From data collected during the dynamic test, five natural frequencies and mode shapes associated with rigid-body and flexural movements of the wagon platform were identified through the Enhanced Frequency-Domain Decomposition (EFDD) method. A detailed 3D finite-element (FE) model of the loaded freight wagon was developed, requiring precise knowledge of the vehicle design details which, in most situations, are difficult to obtain due to confidentiality reasons of the manufacturers. The model calibration was performed through an iterative method based on a genetic algorithm and allowed to obtain optimal values for seven numerical parameters related to the suspension's stiffnesses and mass distribution. The stability of the parameters considering different initial populations demonstrated the robustness of the optimization algorithm. The average error of the natural frequencies decreased from 8.5% before calibration to 3.2% after calibration, and the average MAC values improved from 0.911 to 0.950, revealing a significant improvement of the initial numerical model.

1. Introduction

Over the years, freight railway traffic has experienced progressive growth in transported goods, which consequently leads to an increase in the number of operating trains, speeds and axle loads. These changes are responsible for an increase in the dynamic loads induced by the freight vehicles on the railway infrastructure, potentially affecting the running safety, the stability of the transported goods and durability of the components of vehicle and infrastructure [1–5].

In order to obtain accurate predictions of the dynamic responses, both from the infrastructure and vehicles, advanced train-track dynamic interaction formulations have been developed [6,7]. Delgado and Santos [6] solved the train-track interaction problem adopting an uncoupled formulation, in which equations of motion of both track and vehicle were solved separately through an iterative process until the convergence of the interaction forces was reached. Adopting a distinct approach Montenegro et al. [7] solved the problem using a coupled formulation, based on the Lagrange multipliers method, in which constraint equations of the contact were added to the equations of motion forming a hybrid system of equations. To accurately simulate the contact interface a novel finite element based on Hertz's theory, for the normal contact, and Kalker's laws for the lateral contact, was proposed. The reliability of the dynamic responses obtained with these formulations depend on the accuracy of the numerical models, both from the

* Corresponding author.
E-mail addresses: drr@isep.ipp.pt (D. Ribeiro), cassioscb@ufmg.br (C. Bragança), c.costa@ipt.pt (C. Costa), pfmjorge@fe.up.pt (P. Jorge), rubenfsilva@fe.up.pt (R. Silva), aarede@fe.up.pt (A. Arêde), ruiabc@fe.up.pt (R. Calçada).

https://doi.org/10.1016/j.istruc.2022.01.085
Received 16 August 2021; Received in revised form 23 January 2022; Accepted 29 January 2022
Available online 7 February 2022

vehicle and track, which can be significantly upgraded with the use of dedicated calibration strategies based on site measurements [8,9].

The numerical modelling of the vehicle is typically performed based on two main approaches, multibody [10–13] and finite element method (FEM) formulations [1,14–17]. The first approach considers the vehicle carbody, bogies and wheelsets as rigid elements, connected by spring-dashpot assemblies simulating the suspensions, which are the only flexible components of the model. The inertial properties are provided by concentrated mass elements, including the translational and rotational inertias, and positioned on the gravity center of the vehicle structural components. Due to its simplicity, this approach is computationally very efficient and provide accurate results in terms of global dynamic response of the vehicle, given by the rigid body movements. These movements are associated with translation of the carbody in different directions, as well as its rotation (yaw, pitching and rolling).

Multibody formulations have been widely used by researchers in different applications, such as: i) the design of the vehicle components to resist fatigue, ii) analysis of the vehicle-cargo dynamic interaction including the cargo stability, iii) wheel-rail contact stability under normal and extreme operation conditions, and iv) pantograph-to-catenary contact dynamics.

Hwa Park et al. [10] used a multibody-based dynamic simulation to access the load conditions of a tilting bogie and calculate its fatigue resistance. Zhang et al. [12] developed a multibody model, considering vehicle-cargo coupling, in order to study the cargo stability and access diagonal lashing forces when the vehicle negotiates curves. Different configurations of lashing stiffness and pretension were investigated, concluding that stiffness plays a major role in increasing cargo stability. Peixer et al. [11] performed a parametric study to evaluate the running safety of ICE 3 trains circulating over a viaduct and considering different levels of track irregularities. The safety analysis was based on simulations including the vehicle-track dynamic interaction and using a multibody model for the train. The results obtained for different running safety criteria (Nadal, Prud'homme and Unload criteria) proved that traffic safety was not put at risk for current operating speeds. Antunes et al. [13] developed a 3D multibody model of a pantograph and proposed a numerical tool to study the dynamic behavior on its contact with the catenary. Based on a real case-study of pantograph–catenary interaction in high-speed rail operations, significant differences were found in the dynamic response of the catenary in curved and straight tracks.

On the other hand, the modelling of railway vehicles based on FEM formulations allows to consider the structural flexibility of the vehicle, in particular the influence of global structural modes of the carbody, as well as local modes from specific carbody components (e.g., floor, walls) [14]. The deformability of the vehicle components is usually covered through the use of flexible beam, shell and solid elements, simulating its real geometric and mechanical properties [1]. However, the development of a flexible FE model requires the precise knowledge of the vehicle design, which in most situations is difficult to obtain due to confidentiality reasons of the manufacturers [18]. Also, FEM formulations are usually computationally demanding.

In the last years, FEM-based formulations have been used by researchers in several applications where more detailed information about the vehicle dynamic response is required. Diana et al. [14] demonstrated that considering the flexibility of the carbody and its components is crucial to evaluate passenger comfort. Simulations performed for rigid and flexible vehicle models under similar track conditions showed that the vehicle floor experiences significantly higher acceleration levels when its flexibility is considered. Xue et el. [15] used a flexible carbody model of a freight train to study the influence that different container mounting schemes have on the vertical vibration of the platform. The analysis showed that the stiffness and damping parameters of the container connectors significantly influences the dynamic response of both platform and containers. Liu et al. [16] investigated the influence of considering the carbody flexibility on the fatigue life assessment of a sliding wall covered freight wagon. A parametric study was performed demonstrating a relevant reduction of the expected fatigue life as more modes of vibration were included on the dynamic analysis. Stichel [17] studied the influence of considering the wagon platform flexibility on the hunting motion and concluded that the platform structural modes, especially the first torsional mode, increased the hunting motions.

Obtaining a precise numerical model of a freight wagon is particularly difficult due to constructive and operational specificities of this type of vehicles. In freight wagons, the ratio between laden and tare masses can be as high as 5:1, compared to 1.5:1 in passenger vehicles. Typically, such mass ratios require modelling the wagons under loaded and unloaded conditions [19]. Additionally, the correct positioning of the masses needs to be considered, as it affects the location of the center of gravity of the vehicle and, consequently, its dynamic behavior [20]. To define the center of gravity, the characteristics of the mounting scheme used for the connection between the vehicle platform and the container may be relevant [15]. Also, the motion of the transported cargo, especially in the case of liquids, can influence the behavior of the vehicle. Besides the particular mounting schemes and loading characteristics, freight vehicles are usually equipped with friction suspensions [21], whose behavior is highly nonlinear due to the dry friction damping and motion restrictions [22,23], which also increases the modelling complexity [24].

The use of calibrated models based on dynamic experimental data is particularly relevant to obtain representative models of freight vehicles. Typically, the assessment of vehicle dynamic properties is based on dynamic tests, which can be performed with the vehicle at rest [1,25] or during operation [26–28], but in most cases they are performed in rest conditions. When the vehicle is at rest, the experimental studies are normally performed under a controlled environment, allowing the use of more detailed experimental setups as well as using different types of forced dynamic excitation. The excitation is usually performed using an electrodynamic exciter, impacts from other vehicles, hydraulic actuators, impact hammers or people randomly jumping over the wagon [1]. On the other hand, considering the vehicle in operation, the excitation is mainly provided by the track irregularities [27].

The data collected during the dynamic tests must be processed to identify the modal parameters. Typically, the modal identification techniques are based on input–output [25] or output-only strategies [1,27]. Classical input–output techniques rely on the measurement of the excitation forces (input), as well as the dynamic responses (output), based on Frequency Response Functions (FRFs) [25]. In turn, the output-only techniques, also denominated as Operational Modal Analysis (OMA), do not require the measurement of the excitation forces, but only the dynamic responses, making the test simpler and more accessible. Ribeiro et al. [1] applied a time-domain method, the Stochastic Subspace Identification (SSI), for extracting the natural frequencies and mode shapes of the carbody and bogie of an Alfa Pendular tilting train. Sichani & Ahmadian [27] applied a frequency-domain method, the Frequency Domain Decomposition (FDD), for the modal analysis of a freight vehicle considering both rest and operation conditions. A recent study conducted by Bragança et al. [26] proved the robustness of OMA techniques in estimating the modal parameters of a freight wagon based on limited experimental data. The authors used the information derived from only four measuring points, strategically positioned on the base platform and bogies of the vehicle, for identifying rigid-body mode shapes and natural frequencies associated with bouncing, pitching and rolling movements.

Typically, the calibration of the numerical model of a vehicle involves an iterative adjustment of the numerical parameters until a reasonable agreement is obtained between the numerical and experimental modal parameters [1]. The calibration strategies are generally automatic and based on optimization algorithms that minimize an objective function through successive iterations [26]. Several algorithms can be used to solve the optimization problem, namely gradient-based algorithms, response surface methods and nature-inspired algorithms (e.g., genetic algorithm, evolutionary strategies, particle swarm

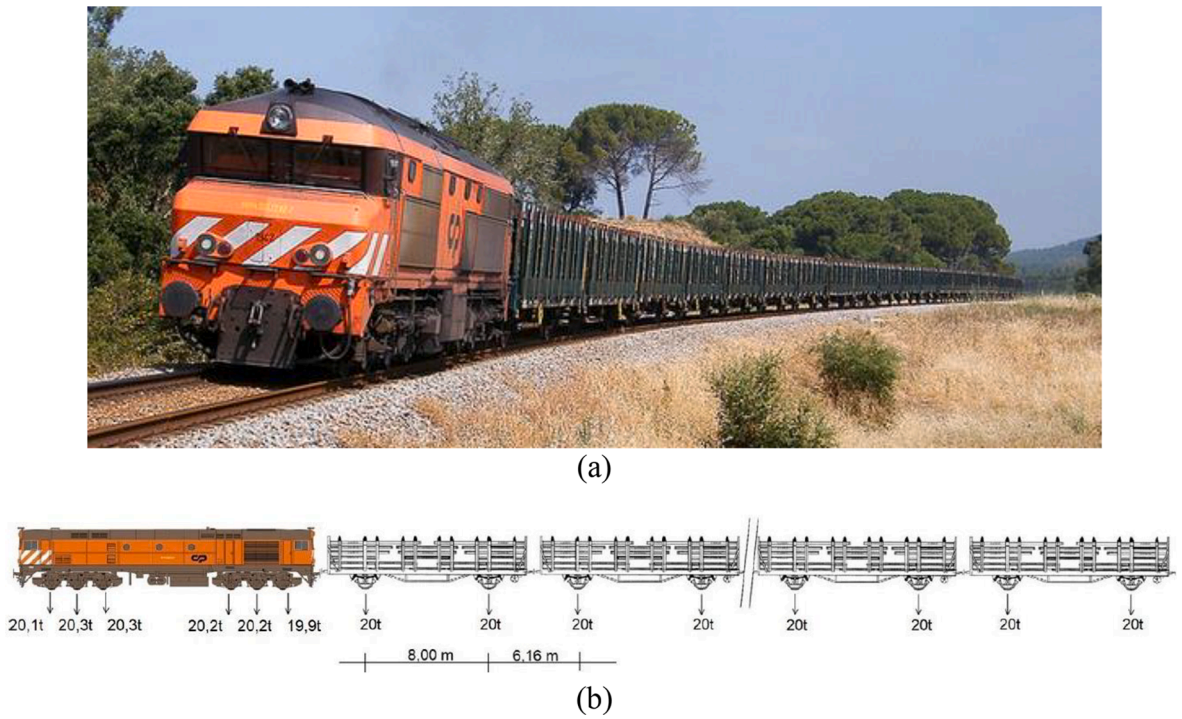

Fig. 1. The freight train: (a) overview, (b) loading scheme.

optimization, etc.). One key aspect for the optimization success is to use a reliable mode pairing technique, i.e., the correspondence between each experimentally obtained mode and a numerically derived mode, to guarantee a fast convergence to the optimal solution [1,29,30]. However, the calibration of railway vehicles numerical models is still a subject scarcely reported in the literature, especially in the case of freight wagons. From the few identified works, most of them are focused on the calibration of passenger's vehicles [1,26,30–33].

In this framework, the present work intends to give valuable contributions to subjects that still need to be enhanced in the existing literature, namely:

- Studies involving the development of detailed 3D FEM models of freight wagons are still scarce if compared to the multibody approach. Furthermore, in most of the existing works the models are based only on data provided by the wagon manufacturers or derived from the literature, which, very often, is imprecise or even not available. This constitutes a major drawback to these studies that could be significantly improved by adopting adequate model calibration techniques. This paper fills both those gaps by providing detailed information on FEM modeling of a freight wagon and further calibrating its properties based on experimental modal parameters;

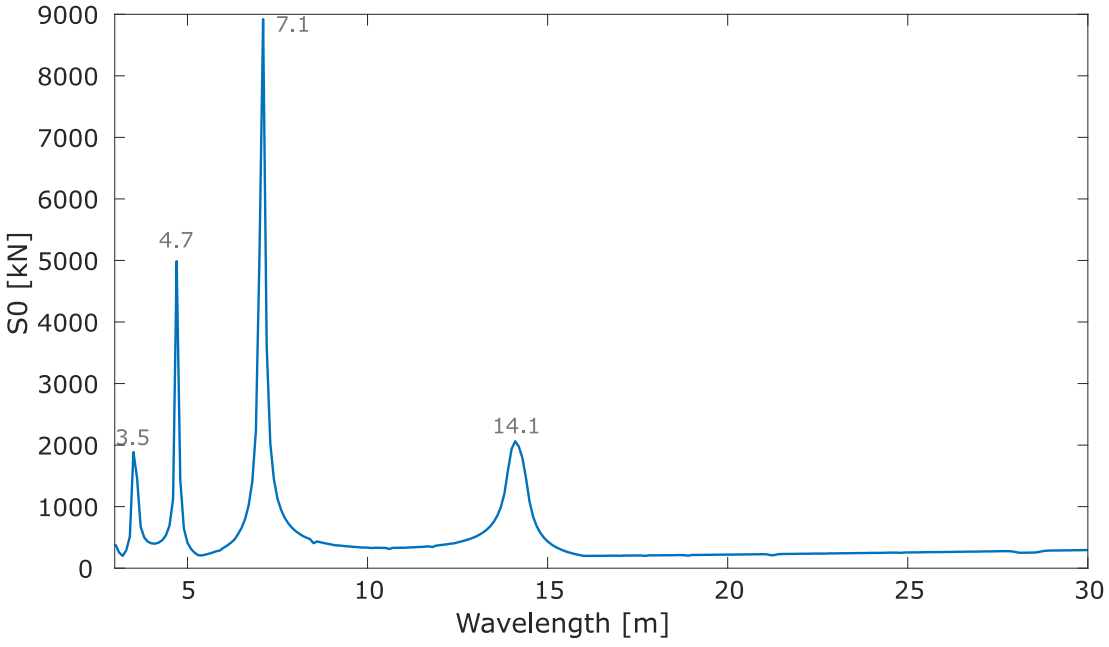

Fig. 2. Dynamic signature of the freight train.

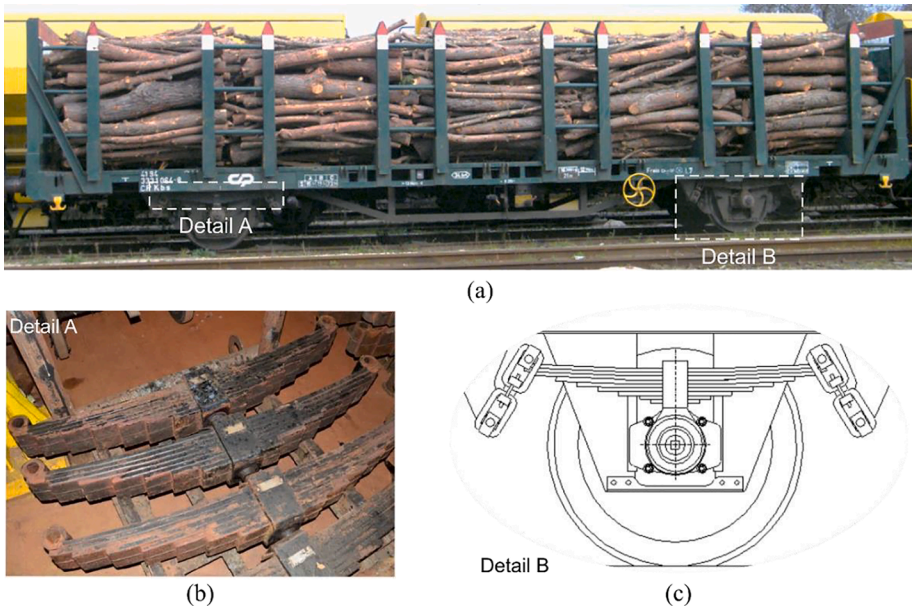

Fig. 3. Kbs wagon: (a) side view (with eucalyptus wood cargo), (b) trapezoidal leaf spring (detail A), (c) primary suspension scheme (detail B) [19].

- Most of the studies regarding the modal identification of railway vehicles, not only are focused on passenger vehicles but also are performed under controlled laboratory conditions, which typically requires the dismantle/adaptation of the vehicle structure for the test setup. This approach is a major issue from the practical point-of-view since normally requires the vehicle to be out-of-service for a long period. In this study the authors proposed an efficient experimental strategy performed during the unloading of cargo and in a time-period compatible with the tight operational schedule of the wagons. Even in these difficult circumstances, the experimental setup allowed to obtain accurate and reliable results, which typically is much more difficult to obtain in tests with the vehicle under operation;
- The calibrated FEM model of a freight wagon under loaded conditions has potential to be used in the dynamic analysis of the train-track system under operational conditions, particularly in evaluating the wheel-rail contact stability as well as the cargo stability. Most of the works envisaging the running safety assessment are based on non-calibrated models and/or models with an insufficient level of detail, which may decisively restrain the conclusions of these studies.

Thus, this article details a complete methodology for the calibration of a complex 3D FE model of a freight vehicle based on dedicated experimental tests. This represents a step forward in the field of railway vehicle dynamics, since the calibrated models derived from the application of model updating techniques, are the basis for obtaining accurate

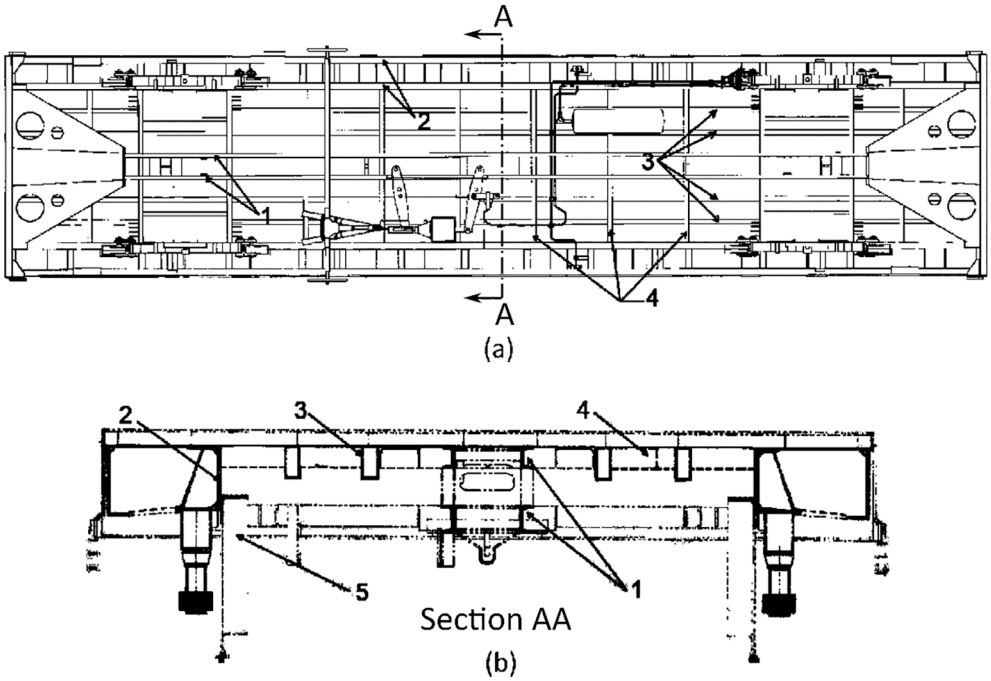

Fig. 4. Structural details of Kbs wagon platform: (a) bottom view, (b) cross section A-A.

Table 1
Main geometrical characteristics of the steel girders of Kbs vehicle platform.

	Girder	Cross section	Profile designation/ dimensions	Geometrical properties		
1	Main - central	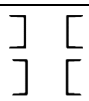	2 U 100x50x6+2 U 120x50x7	Area	0.61 × 10^{-2}	m^2
				I_Y	1.55 × 10^{-4}	m^4
				I_Z	1.89 × 10^{-4}	
				I_t	7.02 × 10^{-8}	
2	Main - lateral		U 320x120x10	Area	0.54 × 10^{-2}	m^2
				I_Y	0.69 × 10^{-5}	m^4
				I_Z	8.02 × 10^{-5}	
				I_t	1.77 × 10^{-7}	
3	Secondary		RECT 160x70x7	Area	0.30 × 10^{-2}	m^2
				I_Y	2.44 × 10^{-6}	m^4
				I_Z	9.37 × 10^{-6}	
				I_t	6.21 × 10^{-6}	
4	Cross girders		RECT 120x70x7	Area	0.25 × 10^{-2}	m^2
				I_Y	1.88 × 10^{-6}	m^4
				I_Z	4.52 × 10^{-6}	
				I_t	4.19 × 10^{-6}	
5	Main – lateral (reinforcement)		C 80x60x5	Area	6.75 × 10^{-4}	m^2
				I_Y	4.43 × 10^{-7}	m^4
				I_Z	2.17 × 10^{-7}	
				I_t	5.52 × 10^{-9}	

and reliable dynamic responses of the train-track system.

2. Freight train

The freight train consists of a diesel-electric locomotive, 1900 series [34] pulling between 20 and 25 timber transport wagons, Kbs series, all identical, and owned by the Portuguese rail transport company Medway. The locomotive has six axles, three axles per bogie, with an axle load equal to approximately 200 kN. In the configuration with 25 wagons, the train has a total length of 370.4 m and can reach a maximum speed of 120 km/h. Fig. 1 (a) shows an overview of the complete freight train and Fig. 1 (b) the corresponding loading scheme.

To better understand the dynamic excitations caused by this freight train, the ranges of wavelengths capable of generating peaks on the dynamic response, Fig. 2 shows the dynamic signatures (S_0) of the 25 wagons composition, considering wavelengths between 3 m and 30 m. The dynamic signature of a train is a reference parameter for representing the dynamic excitation of the train, which depends on the values of axle loads and distance between axles, and can be obtained from the following expression [35]:

$$S_0(\lambda) = \max_{i=1,N} \sqrt{\left[\sum_{k=0}^{i} P_k \cos\left(\frac{2\pi x_k}{\lambda}\right)\right]^2 + \left[\sum_{k=0}^{i} P_k \sin\left(\frac{2\pi x_k}{\lambda}\right)\right]^2} \quad (1)$$

where λ represents the wavelength, P_k the load value of the k axle, x_k is the distance of the k axle to the first axle of the train and N is the number of axles of the train. The peaks identified in Fig. 2 correspond to the wavelengths for which the train is more aggressive and, consequently, more prone to excite the railway infrastructure. Particularly, the wavelength of 14.1 m is related to the distance between groups of two consecutive axles belonging to different wagons. Also, the wavelength of 7.1 m is related to the distance between axles of the same wagon [36]. The identified wavelengths may not correspond to the exact distances between the train axle groups (see Fig. 1b) due to perturbations caused by nearby wavelengths from the locomotive or other characteristic distances of the wagons.

2.1. Kbs wagon

The Kbs vehicle is a freight wagon for timber transport having fixed shafts for the side confinement of the roundwood [34], as presented in Fig. 3. The wagon has a length of 12.78 m per 2.70 m width and rests on two axles spaced apart 8 m. Kbs wagon allows a maximum height of eucalyptus wood of 1.70 m limited to a maximum of 23,700 kg. The average tare weight is 16,300 kg, thus making a total maximum weight of 40,000 kg, which approximately corresponds to a load of 200 kN per axle. The wagon structure is formed by a grid of steel girders supported by UIC standard leaf spring primary suspensions [37].

The vehicle platform is formed by a grid of steel girders, composed of three main longitudinal girders, one at the center (1) and two on the sides (2); secondary girders (3) also in the longitudinal direction; and cross girders (4) disposed of in the transverse direction, as presented in Fig. 4.

Table 1 presents the main geometrical characteristics of the grid of steel girders that constitute the platform of Kbs vehicle. The table includes the numbering of the girders (according to Fig. 4), the cross-section scheme, the dimensions of the profiles and corresponding area and inertial properties.

The girders that most contribute to the overall stiffness of the wagon platform are the two U-profiles forming both lateral main girders (2) and the set of four U-profiles that constitute the central main girder (1). In the case of the lateral girders, between the wagon axles, there is an eccentric reinforcement provided by angles with 8 cm height and positioned approximately 72 cm below the center of gravity of each lateral main girder. In the case of the central girder, the U-profiles are of smaller size but with a spacing of 30 cm between centers of gravity which considerably increase its stiffness. Also, in some sections along its length, additional metallic sheets are coupled to the U-profiles.

At both ends of the wagon, there are closing metallic panels rigidly connected to the top of the platform. The structure of each end panel consists of four vertical columns, with 2.085 m height, and four horizontal bars with 2.840 m width, on which is placed a metallic sheet of 3 mm thickness.

As non-structural elements, there are 10 shafts in H-profile on each side of the vehicle to confine wood. These profiles have an approximate width of 18 cm and develop up to a height of 2.10 m.

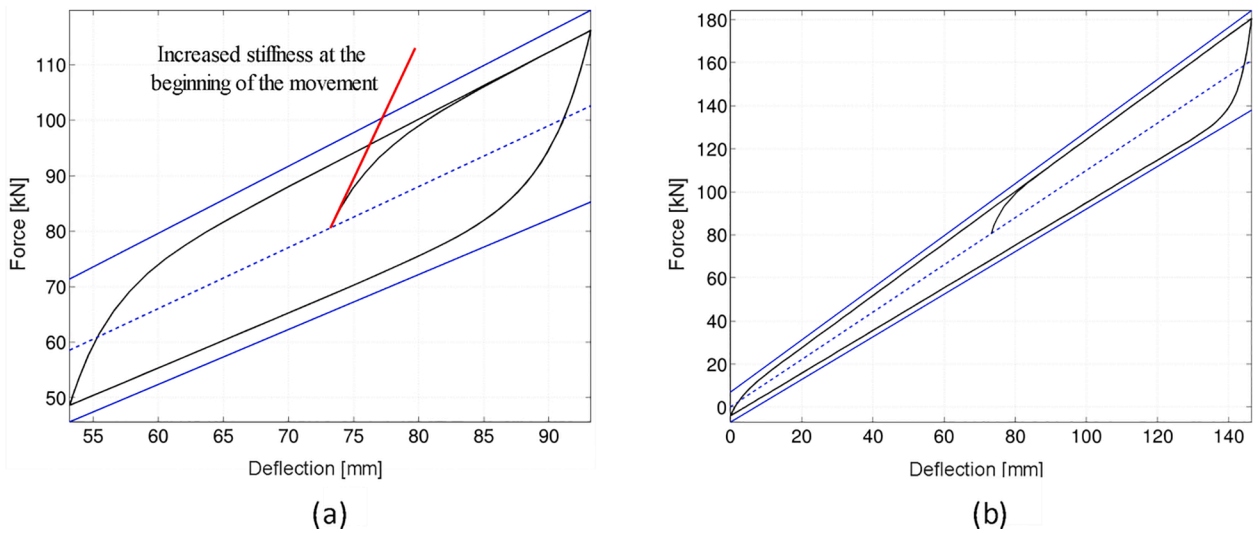

Fig. 5. Hysteretic cycles associated with the behavior of the primary suspensions under harmonic loadings with amplitudes of: (a) 20 mm; (b) 73.2 mm (adapted from [23]).

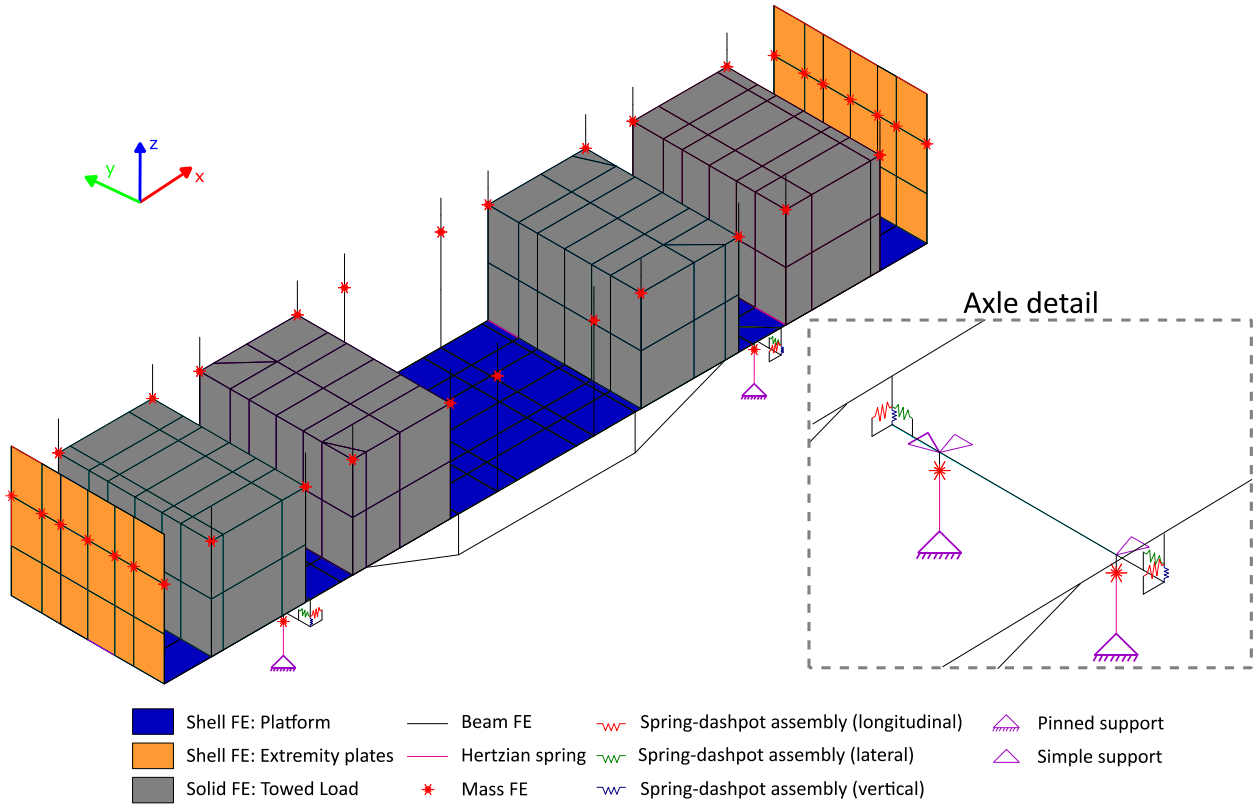

Fig. 6. Kbs wagon numerical model.

2.2. UIC double link suspensions

The Kbs two-axles wagon is equipped with a suspension of the type UIC standard trapezoidal leaf spring [37], which connects the vehicle platform to the axle box. These springs are formed by a set of steel frictional sheets (detail in Fig. 3b) with free rotation at their ends provided by dedicated hinges (UIC links). The springs are composed of nine metal sheets, each one with a thickness of 16 mm, where the first sheet has a length of 1400 mm between connecting hinges. This type of suspension allows relative movements between the vehicle platform and the axle box in the vertical, longitudinal and transversal directions.

The dynamic behavior of the leaf springs suspensions is typically quite complex to model and predict, as shown by many researchers. Works developed by Hoffmann [22,23], True et al. [38], Piotrowski [39], Jönsson et al. [40] and Iwnicki et al. [19] are examples of specific research carried out in leaf spring suspensions applied in the context of modelling the dynamic behavior of freight vehicles. In this type of suspension, the stiffness and damping values vary as a function of the displacement that the spring is subjected due to the imposed loads, as well as lubrication and maintenance conditions. In the vertical direction, the spring stiffness is mainly dependent on the bending stiffness of the set of steel sheets, while the hysteretic damping is associated with the

Table 2
Characterization of the parameters of the numerical model of Kbs wagon.

Parameter	Designation	Adopted value	Limit lower / upper	Unit
D_1	Platform's density (central zone)	77	70 / 85	kN/m^3
D_2	Platform's density (extremities zones)			
K_1	Vertical stiffness of suspension 1	10,000	7,000 / 20,000	kN/m
K_2	Vertical stiffness of suspension 2			
K_3	Vertical stiffness of suspension 3			
K_4	Vertical stiffness of suspension 4			
K_{lat}	Lateral stiffnesses of suspensions 1 to 4	500	400 / 700	kN/m
K_{long}	Longitudinal stiffnesses of suspension 1 to 4			
E_s	Steel deformability modulus	210	180 / 230	GPa
M_{ext}	Admass on extremities plate (per node)	70	60 / 300	kg
M_{lat}	Admass on lateral shafts (per node)			
C_{susp}	Damping of suspensions	34.0	- / -	kN.s/m
K_{Hertz}	Stiffness of the Hertzian wheel-rail contact	1.53x10^6	- / -	kN/m

dry friction developed between the metallic sheets.

Hoffman [22] proposed a methodology to characterize the hysteretic loop of the UIC double link suspensions [37], which is presented in Fig. 5. From the hysteretic loop, it is important to highlight the high apparent stiffness at the beginning and when the motion changes its direction. This aspect can be seen from the red tangent line in Fig. 5 (a) and every time the system reaches its maximum or minimum displacement. Subsequently when the system begins to move the slope of the curve becomes less intense until it stabilizes at its nominal value of 1,000 kN/m. This behavior is caused by static friction between the metal sheets which, while not broken, causes the system to flex as a single body with extremely high stiffness. After the friction is broken, the sheets can slide, reducing the apparent stiffness of the system.

3. Numerical modelling

3.1. Description

The three-dimensional finite element model developed for Kbs wagon and developed in ANSYS® software [41] is presented in Fig. 6. The geometry of the wagon, as well as the cross sections of the structural elements, were derived from the design drawings (Table 1) and complemented by visual inspections. The vehicle model had its movements restrained at the wheel-rail contact point and on both axles. In case of the axles rigid supports were added to block the translations on the transversal and longitudinal directions, as well as the rolling and yaw rotations.

The girders of the platform (central, lateral and cross girders), as well as the columns and horizontal bars located on the panels of both extremities of the wagon, were modelled by beam finite elements (BEAM188). The metallic sheets of the base platform and extremity plates were modelled using shell finite elements (SHELL181). The primary suspensions were modelled by spring-dashpot assemblies (COMBIN14) in the vertical, lateral and longitudinal directions. The vehicle axles and the lateral shafts were simply modelled through rigid beam elements. The wheel-rail contact is modelled by a spring-dashpot assembly (COMBIN14) which stiffness is estimated from the Hertz contact theory [42]. The masses of the lateral shafts, wheels and side elements were modelled by mass elements (MASS21). The masses of the extremity plates and lateral shafts were simply applied at 2/3 of the height. The tare weight of the vehicle was tuned considering an equivalent density for the base platform, which may be different in the central zone (between axles) and extremities zones (between axles and vehicle ends). The eucalyptus towed loads were modelled by solid elements (SOLID185). The modulus of elasticity of the eucalyptus wood was considered equal to 15.2 GPa and the density equal to 650 kg/m^3, considering an average humidity level of 12% [43].

The developed numerical model considered the towel load configuration (load values and layout), similar to the one used during the dynamic test of the Kbs wagon (Section 4).

Table 2 lists the geometric and mechanical parameters of the numerical model of the Kbs wagon, including its designation, the adopted value and the respective unit. Additionally, the lower and upper limits of some of the parameters that will be used in the model calibration phase (Section 5) are listed.

Considering the dynamic vibration test performed on the wagon, which is presented in Section 4, the provided source of excitation was not sufficient to cause significant displacements on the suspensions. Thus, given the hysteretic cycles presented in Fig. 5 a higher stiffness of the suspensions of the order of 10,000 kN/m is expected for the vehicle under these excitation conditions. The vertical stiffness of each suspension spring, represented by the parameters K_1 to K_4, was considered independent since there is no guarantee that all the leaf springs have the same conservation state. The density adopted for the central zone (D_1) and extremities zones (D_2) were constrained to guarantee that the tare weight of the vehicle is fulfilled.

3.2. Modal parameters

Fig. 7 depicts the first 5 numerical mode shapes and corresponding natural vibration frequencies, estimated through a numerical modal analysis performed on the developed FE model. The figure presents a lateral view complemented with a front view per each modal configuration.

The modal configurations involve structural and rigid body movements of the vehicle platform. Modes 1 and 5 are structural modes associated with bending and torsion movements of the vehicle platform. In turn, modes 2, 3 and 4, are associated with rigid body rotations of the vehicle platform, involving the pitching, bouncing and rolling movements, respectively.

4. Dynamic test

This section describes the dynamic test performed on Kbs wagon conducted at The Navigator Company (ex-Soporcel) facilities, in Figueira da Foz (Portugal), aiming to identify modal parameters of the freight wagon. The test was carried out overnight during the train unloading operation without causing a disturbance to its tight schedule of operations. These conditions imposed some restrictions on the test, especially regarding the time window available for carrying out the work, sensor positioning and system excitation.

4.1. Measurement setup

The freight car was instrumented with 16 high-sensitivity piezoelectric accelerometers, PCB model 393B12, with a sensitivity equal to 10 V/g, a measurement range of ± 0.5 g and a frequency range of 0.15–1000 Hz. The response was evaluated in terms of the accelerations in the transverse (y) and vertical (z) directions in one setup, totalizing 14 measurement points (1 to 14). The accelerometers were attached to the carbody using metallic angles fixed to the vehicle with magnetic disks. The PC, data acquisition system (DAQ) and battery supplying system were located in the center of the vehicle. Fig. 8 shows a view of the installed experimental setup on the wagon, as well as some details of the DAQ and the accelerometer connection to the vehicle's platform.

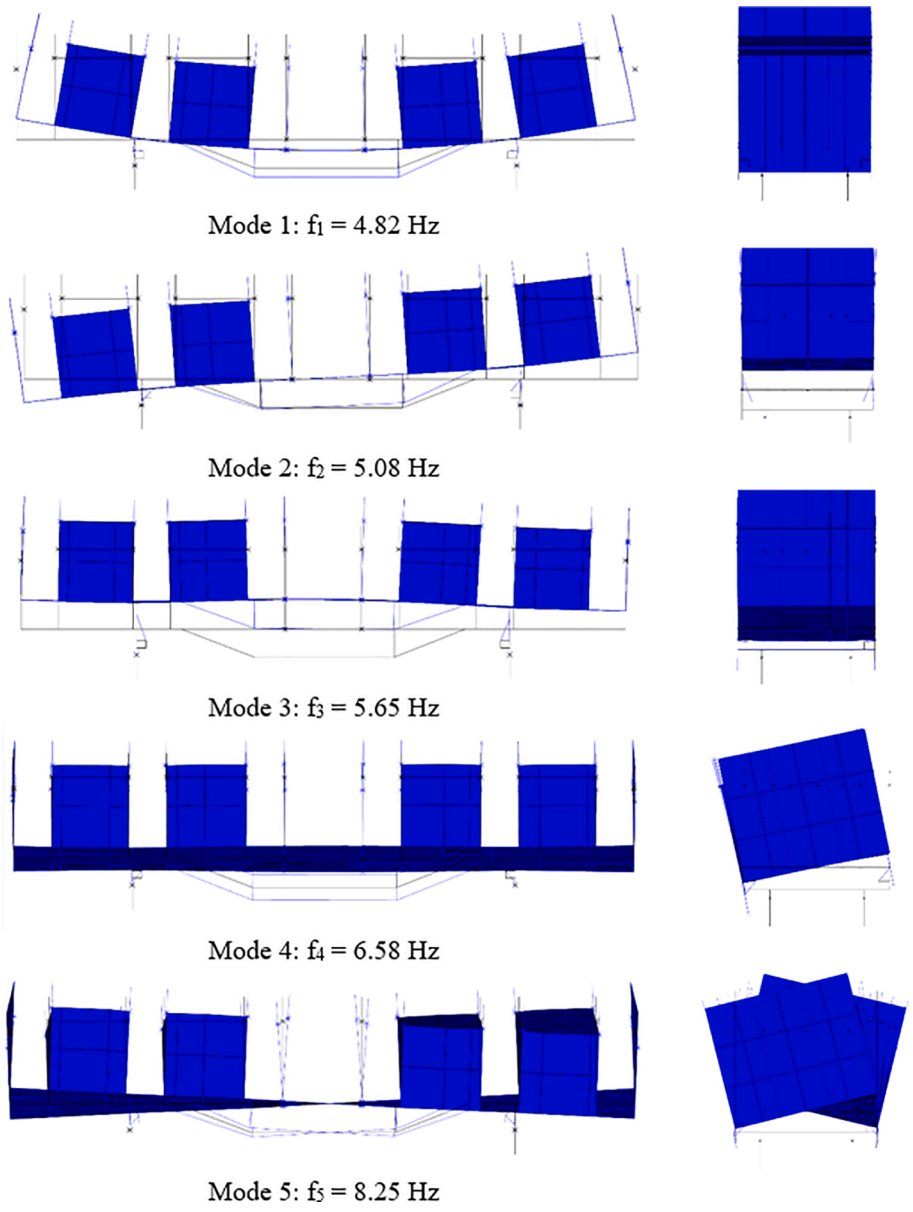

Fig. 7. Main numerical modal parameters of the Kbs wagon.

The data acquisition was performed through the cDAQ-9172 system using four modules NI 9233 for IEPE type accelerometers. The time series were acquired for 10 min periods, with a sampling frequency of 2048 Hz, posteriorly decimated to a frequency of 256 Hz.

During the dynamic test the vehicle was at slow and intermittent motion, practically at rest, and therefore, a random external excitation, in time and space, was required to increase the vibration levels. The excitation was provided by means of a group of people jumping on the edges of the platform. This technique guarantees higher signal-to-noise ratios and consequently an increase of the coherence between the measured signals.

The dynamic test was carefully planned to minimize the influence of noise in the measurements, which involved the use of shielded cables, insulated cable connectors, stable DC power-supply from electrical batteries, denoise filters in the A/D conversion process and high-sensitivity accelerometers.

The test was performed considering the loaded vehicle, however, the central stowage of timber was removed to allow the space needed for the installation of the data acquisition system (Fig. 9a). The option of removing the central stowage, to detriment of the others, was to maintain a symmetrical mass distribution on the wagon. This is important since non-symmetric mass layouts can modify much more pronouncedly the modal configurations, as well as the natural frequencies values, particularly in freight vehicles where the overload/tare mass ratio is high. Additionally, non-symmetric mass layouts are normally less representative of the real operating conditions of Kbs wagons. This dedicated loading configuration will have no influence on the accuracy of the modal parameters' estimation (only in their values), however, conditioned the baseline scenario for which the model calibration will be performed (see Section 5).

Fig. 9 (b) presents a schematic representation of the loading configuration during the dynamic test and the corresponding mass values for each stowage, weighted after the test. The weight on the central stowage was only due to people and equipment, which is considerably lower in comparison to the total overload.

4.2. Modal identification

The identification of the vehicle modal parameters, particularly the natural frequencies, mode shapes and damping coefficients, was

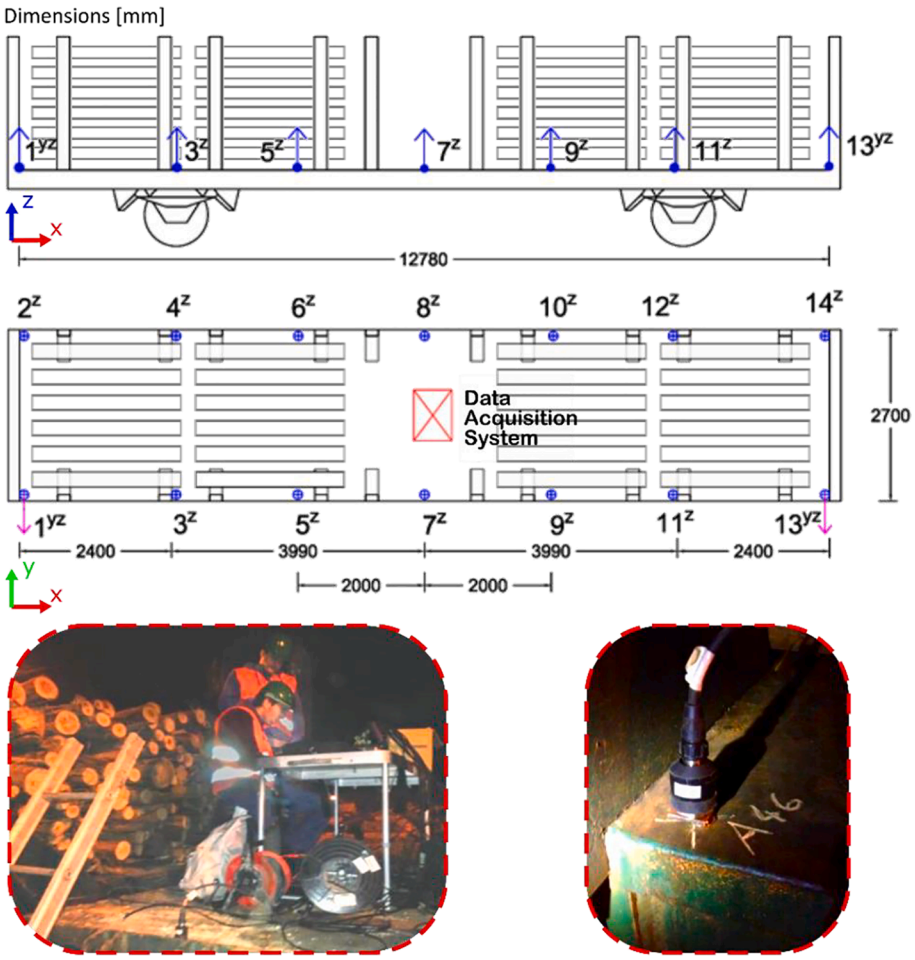

Fig. 8. Experimental test setup of freight wagon *Kbs*.

performed on the ARTeMIS® software [44] using the EFDD (Enhanced Frequency Domain Decomposition) method. EFDD method is a frequency-domain technique that estimates the modal parameters based on a Singular Value Decomposition (SVD) of the estimated spectral density matrices of the measured responses. Fig. 10 shows the average and normalized singular values of the spectral matrices derived from the application of the EFDD method. This allowed to identify 5 natural frequencies, and corresponding operational modal configurations of the wagon, whose peaks are identified on the figure by black dash-dot lines.

Fig. 11 presents the five operational mode shapes identified and the corresponding average values of the natural frequencies and damping coefficients. The deformed modal configurations are represented by red lines and the undeformed mesh by grey lines.

The first two modes involve bending movements of the vehicle platform, with frequencies equal to 5.10 Hz and 5.69 Hz, the third and fourth modes are rigid body modes, associated with bouncing and rolling motions respectively, with frequencies equal to 6.38 Hz and 7.56 Hz, and finally, the fifth mode with a frequency of 8.11 Hz is associated with torsion motion of the vehicle platform. The five identified operational mode shapes are in correspondence with the five numerical mode shapes presented in Fig. 7. The presence of flexural bending modes with frequency values lower than the ones associated with rigid body modes is typical in freight vehicles. This is essentially due to the stiffer primary suspensions, in comparison to the passenger vehicles, as well as the inexistence of secondary suspensions.

The low values of damping coefficients, between 0.46% and 1.36%, are consistent with the vehicle resting/low motion scenario in which the dynamic test was performed and since the provided excitation was insufficient to induce large suspension movements. Although these values of damping are in agreement with the tested scenario, they should not be considered for analyzing the vehicle response under a running scenario, since during operation the suspensions are subjected to much larger displacements and, consequently, the suspensions would provide higher damping.

5. Calibration

The calibration of the numerical model of the Kbs wagon was based on the results of the dynamic test and involved two stages: a sensitivity analysis and an optimization process based on a genetic algorithm.

5.1. Sensitivity analysis

The sensitivity analysis allows for the selection of the numerical parameters that most influence the modal responses (i.e., the five natural frequencies, f_1 to f_5, and five modal configurations, through MAC parameters MAC 1 to MAC 5) and therefore should be included in the subsequent optimization phase. In this study, 11 numerical parameters were selected and stochastically sampled by the Latin Hypercube method. The samples were generated based on a multivariate uniform distribution with the limits of each parameter given in Table 2. The masses of the timber load were not considered as calibration parameters since their values were accurately evaluated during the dynamic test (see Section 4.1).

Fig. 12 shows the results of the global sensitivity analysis in the form of a Spearman's linear correlation matrix based on 1,000 samples

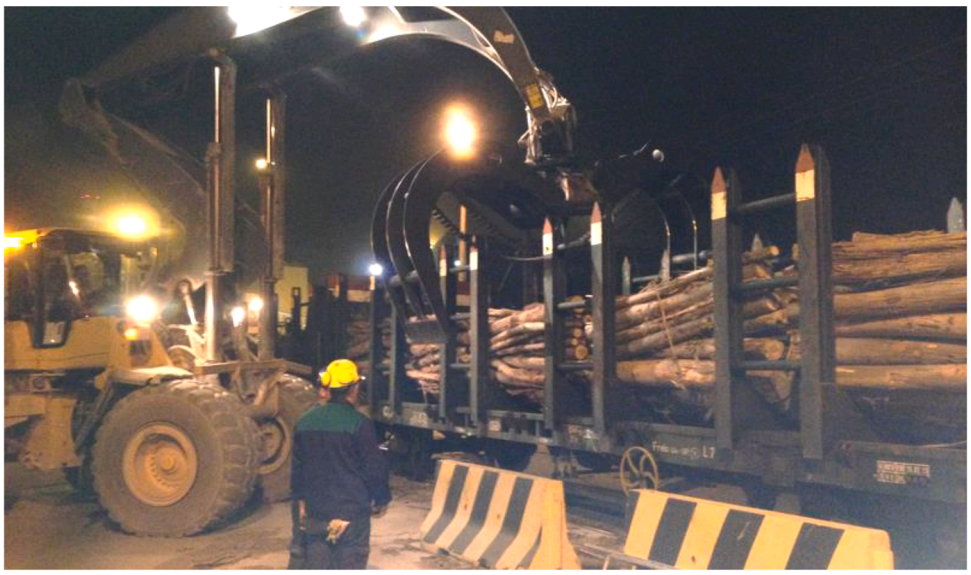

(a)

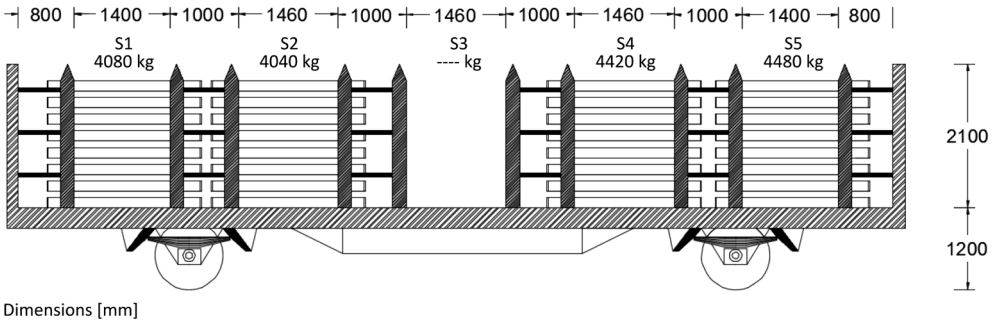

(b)

Fig. 9. Loading configuration during the dynamic test: (a) removal of the central stowage, (b) overload values and distribution.

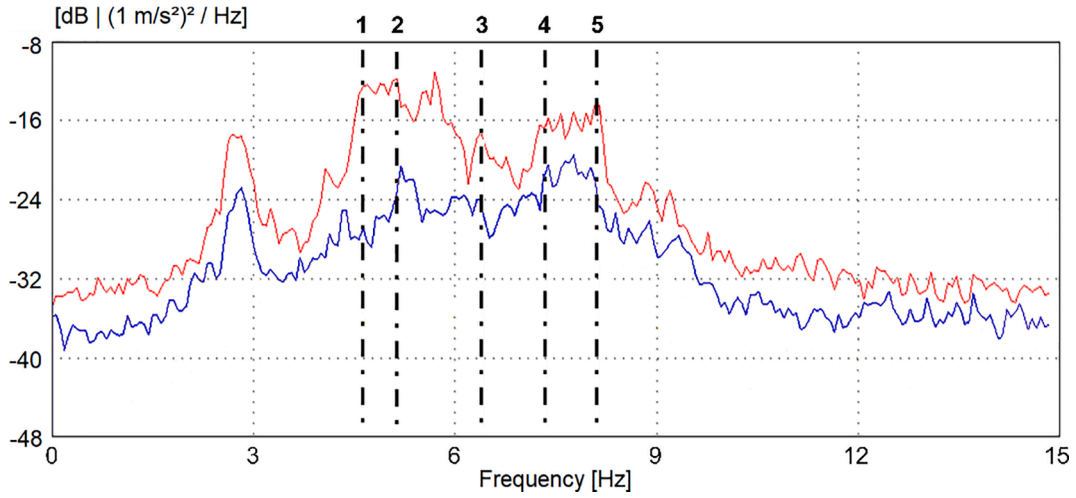

Fig. 10. EFDD method: average and normalized singular values of the spectral density matrices and identified operational modes.

obtained with Latin hypercube sampling method. The samples with a MAC value lower than 0.50 have been excluded from the total amount of samples, as they may represent samples for which the pairing between numerical and experimental mode shapes have failed. Additionally, the samples with a correlation coefficient within the range −0.30 to + 0.30 have been removed from the graphical representation. This strategy

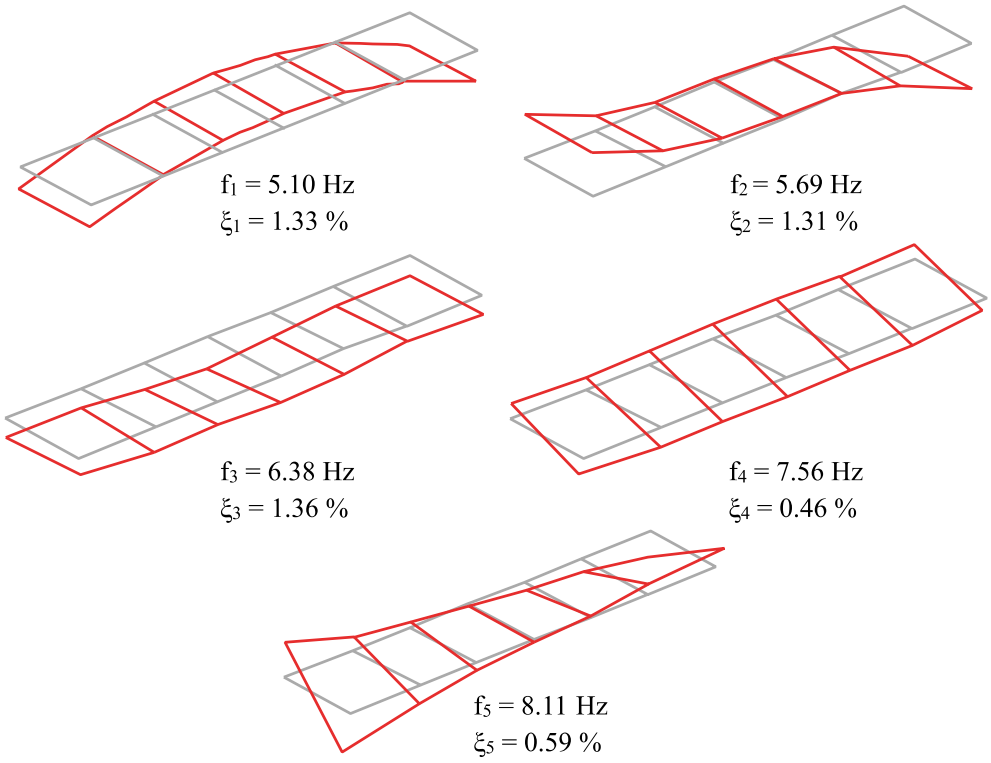

Fig. 11. Experimental modal parameters.

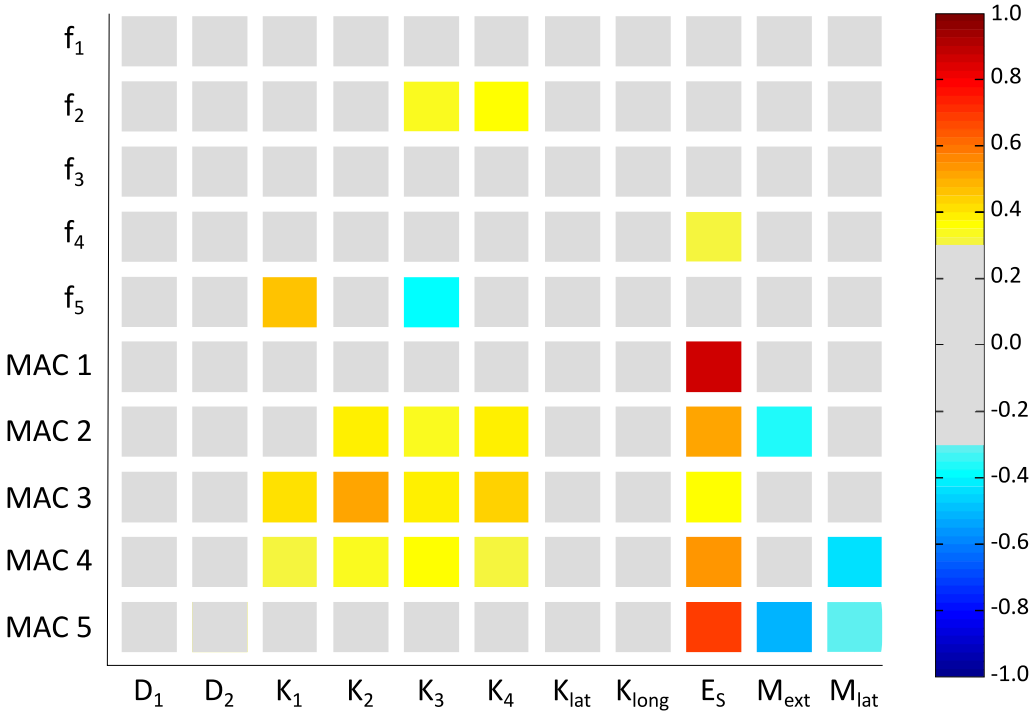

Fig. 12. Spearman's linear correlation matrix.

allows to properly identify the parameters only with a significant amount of correlation with the modal responses.

The sensitivity analysis revealed that from the 11 numerical parameters evaluated, 7 of them have proved to influence the modal responses, particularly, the vertical stiffnesses of the suspensions (K_1 to K_4), the steel deformability modulus (E_S), and the additional masses on the extremities plates (M_{ext}) and lateral shafts (M_{lat}).

The stiffness values of each suspension showed sensitivity enough to be properly estimated in the optimization stage. This is particularly relevant, since in other studies (e.g., [1;26]) the estimation of the suspension stiffness required grouping the suspension parameters, by considering two or even four springs, because the individual stiffnesses presented low correlation values.

Curiously, both densities from the platform (D_1 and D_2) showed

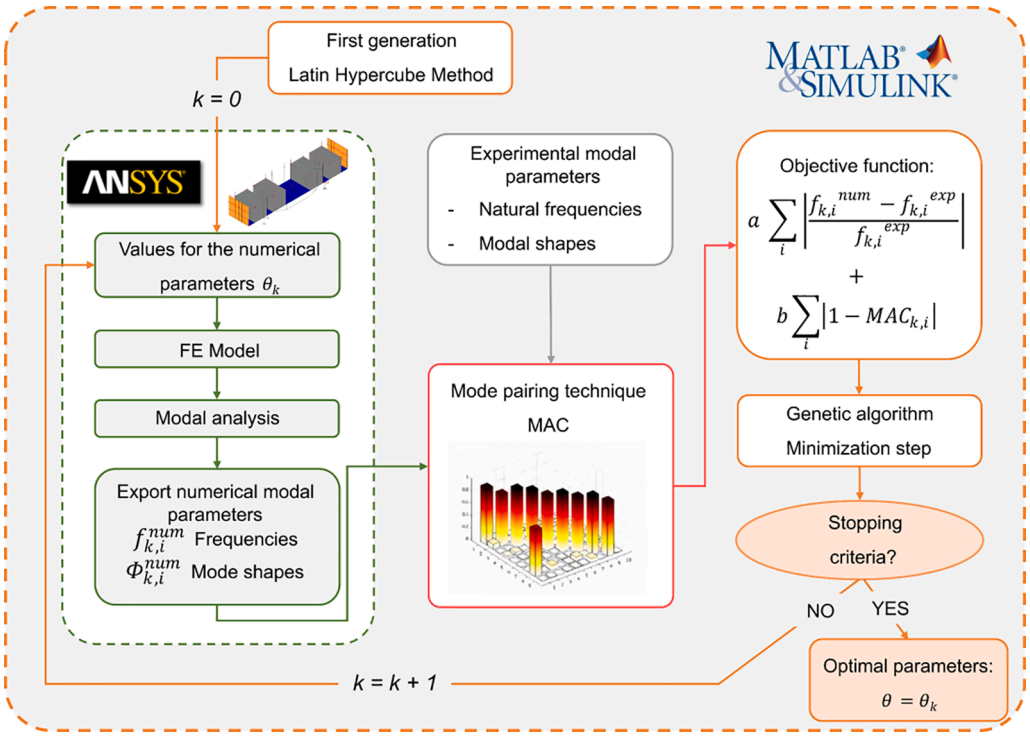

Fig. 13. Calibration process flowchart.

small sensitivity to the modal response, probably due to the symmetry/almost symmetry of the vibration modes, which means that a variation (within the predefined limits) on the position of the masses will predictable not affect its symmetrical configuration.

The lateral and longitudinal stiffnesses of the suspensions (K_{long} and K_{lat}) also showed low sensitivity, which may be justified by the small modal displacements in these specific directions, with mode shapes involving movements mainly in the vertical direction.

5.2. Optimization

The optimization of the numerical model was performed using an

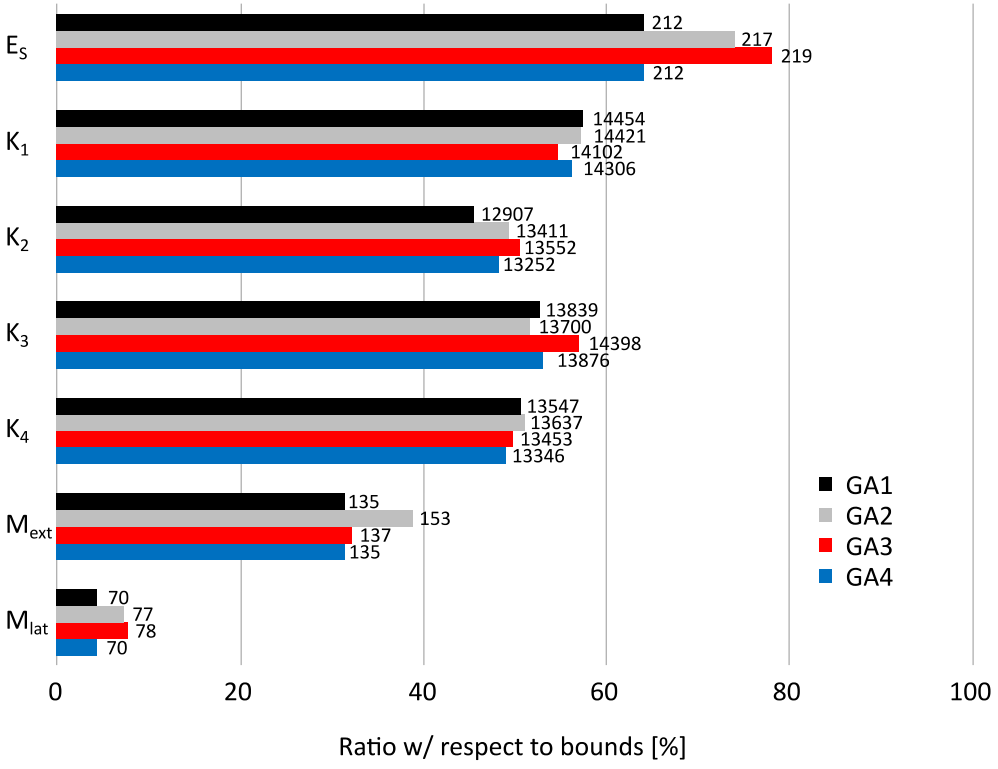

Fig. 14. Values of the numerical parameters for the optimization runs GA1–GA4.

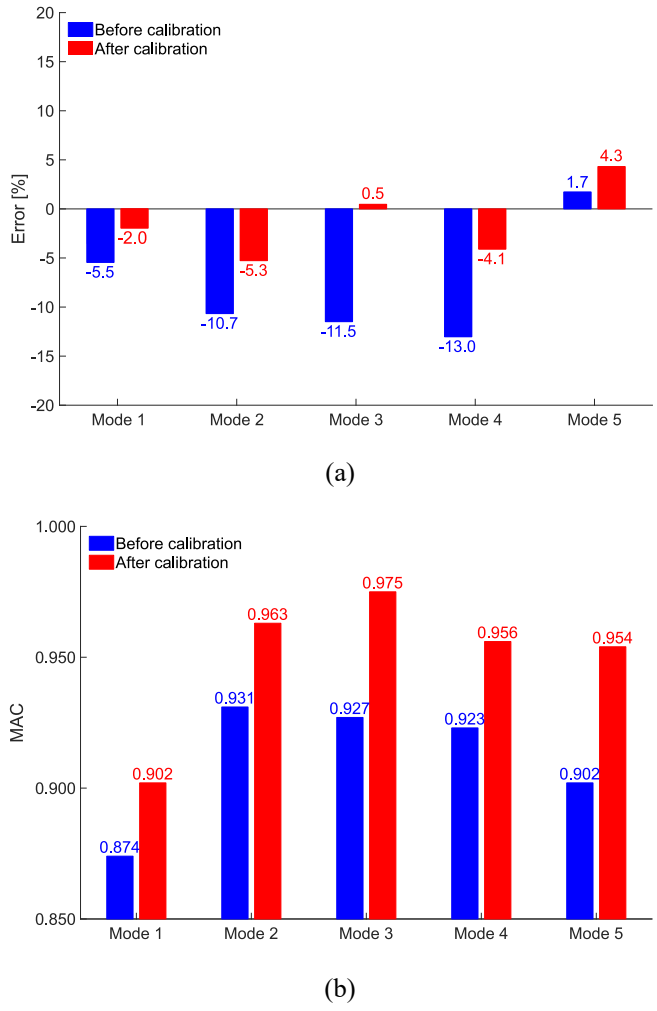

Fig. 15. Errors between experimental and numerical modal responses, before and after calibration: (a) natural frequencies, (b) MAC.

iterative methodology based on a genetic algorithm. The implementation strategy adopted relied on the interaction between two commercial software, MATLAB® [45] and ANSYS® [41], as presented in Fig. 13.

Firstly, in ANSYS® [41], a numerical model is developed based on a set of initial numerical parameters randomly generated by the Latin Hypercube method, within the bounds presented in Table 2 for each parameter. After that, a modal analysis is performed in ANSYS® [41] and natural frequencies and mode shapes are exported to MATLAB® [45] through text files. The mode pairing technic was implemented in MATLAB® [45] based on the MAC correlation matrix calculated between the experimental and numerical mode shapes, in which the rows are associated with the experimental modes and the columns with the numerical modes [46]. The mode pairing is performed, associating each experimental mode with the correspondent numerical mode based on the highest MAC value of each row of the matrix. Finally, a new set of numerical parameters is estimated using a genetic algorithm aiming to minimize the residuals of an objective function. This process is repeated until the maximum number of iterations is reached.

The optimization aimed to find optimal values for 7 numerical parameters based on 10 modal responses values (5 natural frequencies and 5 MAC values). The level of agreement between numerical and experimental modal responses was derived from the following objective function (f):

$$f = a\sum_{i=1}^{5}\left|\frac{f_i^{exp} - f_i^{num}}{f_i^{exp}}\right| + b\sum_{i=1}^{5}\left|1 - MAC(\phi_i^{exp}, \phi_i^{num})\right| \quad (2)$$

where a and b are the residuals weights assumed equal to 1.2 and 0.8 respectively, f_i^{exp} is the vibration frequency of the i^{th} experimental mode, f_i^{num} is the vibration frequency of the i^{th} numerical mode and $MAC(\phi_i^{exp}, \phi_i^{num})$ is the MAC value between the i^{th} numerical and experimental modal configurations.

The selection of the weights must consider the level of uncertainties associated with the experimental estimation of the natural frequencies and mode shapes [47]. Since the natural frequencies were more rigorously estimated than the mode shapes the corresponding weight is higher which allowed to give more importance to the frequencies' residual.

The iterative process started with an initial population of 30 individuals, randomly generated by Latin Hypercube method, whose size has been maintained over 80 generations, totalizing 2,400 individuals. It was considered, a crossing rate of 50%, a number of elites equal to 1 and a mutation rate of 15 % with standard deviation varying linearly from 10 % to 1 % from the first to the last generation.

The optimal values of the parameters were obtained based on the results of four independent optimization runs (GA1–GA4) with different initial populations. Fig. 14 presents the ratio of values of each numerical parameter relative to the bounds indicated in Table 2 for optimization runs GA1–GA4. A ratio of 0% coincides with the lower bound and 100% coincides with the upper bound. Also, the value of each numerical parameter is presented.

In a general overview, all the values from the numerical parameters remained stable with variations below 10%, except for the deformability modulus of steel. However, this larger variation is essentially due to the very limited variation bounds considered for this specific parameter. The results also allow concluding that none of the parameters reached their lower or upper bounds, which shows the robustness and efficiency of the optimization process in the parameters values estimation.

Fig. 15 (a) shows the error values between numerical and experimental frequencies, before and after calibration, taking as reference the values of the experimental frequencies. The results after calibration refer to the optimization run GA4, which is associated with the lowest residual of the objective function. The absolute error of the frequencies was considerably reduced for all the modes, except for the 5th mode in which the error slightly increased. However, the average error of the frequencies decreased from 8.5%, before calibration, to 3.2% after calibration.

Fig. 15 (b) shows a comparison of the MAC values between numerical and experimental mode shapes, before and after calibration. The average MAC value improved from 0.911, before calibration, to 0.950 after calibration.

Fig. 16 presents a comparison of the experimental and numerical modal parameters after calibration considering the optimization run GA4. A nearly perfect match can be observed for the five mode shapes.

6. Conclusions

This paper presents an automatic model calibration methodology of a timber log freight wagon based on experimental modal parameters estimated from a dynamic test performed during the train unloading operation.

The application of a modal identification technique based on the EFDD method allowed to identify five operational modes associated with rigid body and flexural movements of the vehicles platform. The value of frequency from the vertical bending mode (5.10 Hz) was lower than the rigid body mode associated with bouncing motion (6.38 Hz). This order of the modes is significantly conditioned by the high values of the vertical stiffness of the primary suspensions and by the inexistence of a secondary suspension system.

A detailed 3D FEM based model of the wagon was developed in ANSYS® software, based on the original design drawings of the train manufacturer, field observations and data gathered from the literature.

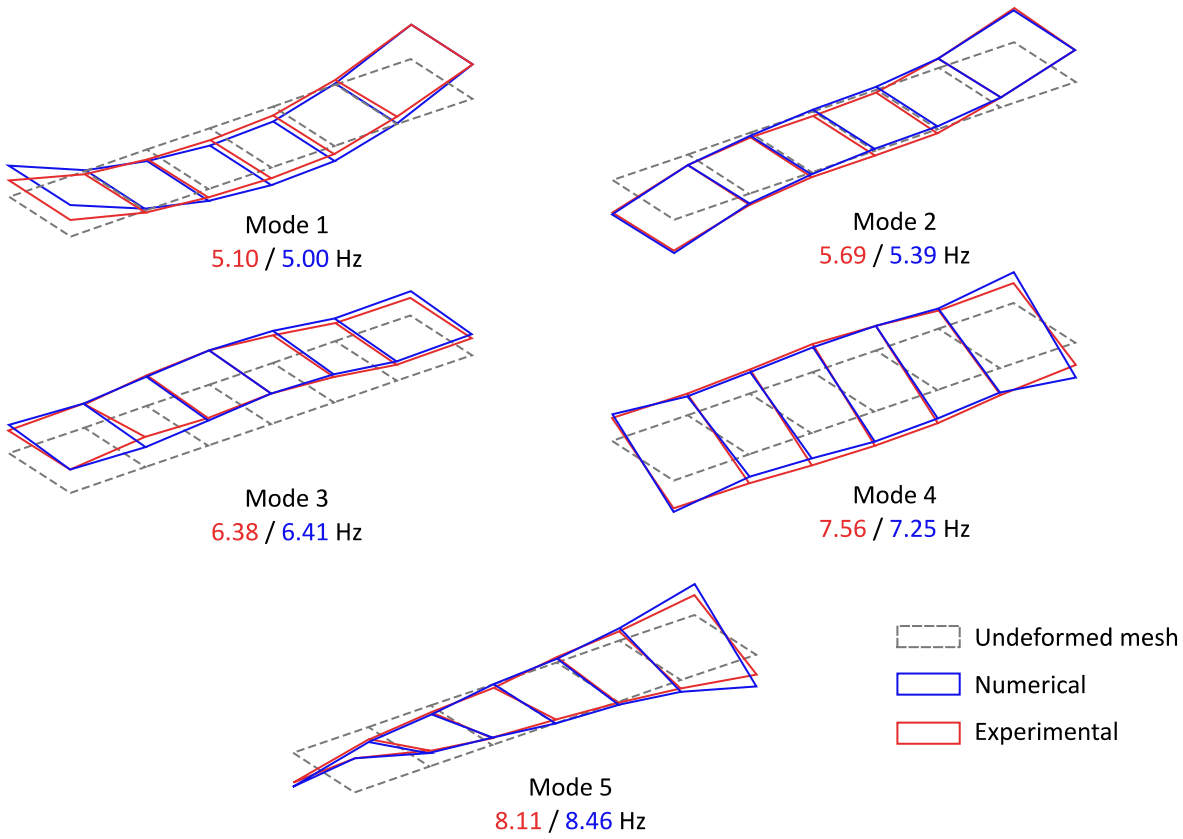

Fig. 16. Comparison between the experimental and numerical, after updating, modal parameters.

The model calibration based on modal parameters involved a sensitivity analysis and an optimization. The sensitivity analysis allowed the selection of seven numerical parameters that most influence the modal responses, namely, the vertical stiffnesses of the suspensions, the steel deformability modulus, and the additional masses on the extremities plates and lateral shafts. The values of sensitivity obtain to the stiffness of the primary suspensions allowed to study them individually. In existing studies, this was not always achieved, or in most cases required a dedicated test layout to obtain experimental data capable of enhancing the sensitivity values of this parameter. The optimization was performed by an iterative methodology based on a genetic algorithm and resorting to an efficient interaction between MATLAB® and ANSYS® software. The stability of the parameters' estimates considering different initial populations demonstrated the robustness of the algorithm. Also, the comparison of experimental and numerical responses before and after calibration revealed significant improvements in the numerical model and a very good correlation between the experimental and numerical responses after calibration. The average error of the natural frequencies decreased from 8.5% before calibration to 3.2% after calibration, and the average MAC values improved from 0.911 to 0.950.

In further studies, the updated numerical model of the freight wagon will be used in the analysis of the vehicle-cargo dynamic interaction, including the cargo stability assessment, as well as for evaluating the wheel-rail contact stability under extreme operation scenarios, namely under strong cross-winds and seismic actions.

Declaration of Competing Interest

The authors declare that they have no known competing financial interests or personal relationships that could have appeared to influence the work reported in this paper.

Acknowledgements

The authors would like to acknowledge the support of the Base Funding UIDB/04708/2020 and Programmatic Funding UIDP/04708/2020 of the CONSTRUCT (Instituto de I&D em Estruturas e Construções) funded by national funds through the FCT/MCTES (PIDDAC). The authors also express their gratitude to Dr. Nuno Pinto and Mr. Valdemar Luís, both technicians of LESE laboratory, for their indispensable assistance during the preparation and execution of the experimental test.

References

[1] Ribeiro D, Calçada R, Delgado R, Brehm M, Zabel V. Finite-element model calibration of a railway vehicle based on experimental modal parameters. Veh Syst Dyn 2013;51(6):821–56. https://doi.org/10.1080/00423114.2013.778416.
[2] Malveiro J, Sousa C, Ribeiro D, Calçada R. Impact of track irregularities and damping on the fatigue damage of a railway bridge deck slab. Struct Infrastruct Eng 2018;14(9):1257–68. https://doi.org/10.1080/15732479.2017.1418010.
[3] Kovalev R, Lysikov N, Mikheev G, Pogorelov D, Simonov V, Yazykov V, et al. Freight car models and their computer-aided dynamic analysis. Multibody Syst Dyn 2009;22:399–423. https://doi.org/10.1007/s11044-009-9170-6.
[4] Arvidsson T, Karoumi R. Modelling alternatives in the dynamic interaction of freight trains and bridges. Civil-Comp Proc 2014;104. https://doi.org/10.4203/ccp.104.65.
[5] Alves V, Meixedo A, Ribeiro D, Calçada R, Cury A. Evaluation of the Performance of Different Damage Indicators in Railway Bridges. Procedia Eng 2015;114:746–53. https://doi.org/10.1016/j.proeng.2015.08.020.
[6] Moreno Delgado R, dos Santos R.C. SM. Modelling of railway bridge-vehicle interaction on high speed tracks. Comput Struct 1997;63(3):511–23. https://doi.org/10.1016/S0045-7949(96)00360-4.
[7] Montenegro PA, Neves SGM, Calçada R, Tanabe M, Sogabe M. Wheel-rail contact formulation for analyzing the lateral train-structure dynamic interaction. Comput Struct 2015;152:200–14. https://doi.org/10.1016/j.compstruc.2015.01.004.
[8] Malveiro J, Ribeiro D, Sousa C, Calçada R. Model updating of a dynamic model of a composite steel-concrete railway viaduct based on experimental tests. Eng Struct 2018;164:40–52. https://doi.org/10.1016/j.engstruct.2018.02.057.
[9] Meixedo A, Ribeiro D, Calçada R, Delgado R. Global and local dynamic effects on a railway viaduct with precast deck. Civil-Comp Proc., vol. 104, 2014. https://doi.org/10.4203/ccp.104.77.

[10] Hwa Park B, Po Kim N, Seok Kim J, Yong Lee K. Optimum design of tilting bogie frame in consideration of fatigue strength and weight. Veh Syst Dyn 2006;44(12): 887–901. https://doi.org/10.1080/00423110600737106.
[11] Peixer MA, Montenegro PA, Carvalho H, Ribeiro D, Bittencourt TN, Calçada R. Running safety evaluation of a train moving over a high-speed railway viaduct under different track conditions. Eng Fail Anal 2021;121:105133. https://doi.org/10.1016/j.engfailanal.2020.105133.
[12] Zhang D, Tang Y, Clarke DB, Peng Q, Dong C. An innovative method for calculating diagonal lashing force of cargo on railway wagons in a curve alignment. Veh Syst Dyn 2021;59(3):352–74. https://doi.org/10.1080/00423114.2019.1686160.
[13] Antunes P, Ambrósio J, Pombo J, Facchinetti A. A new methodology to study the pantograph–catenary dynamics in curved railway tracks. Veh Syst Dyn 2020;58(3): 425–52. https://doi.org/10.1080/00423114.2019.1583348.
[14] Diana G, Cheli F, Collina A, Corradi R, Melzi S. The development of a numerical model for railway vehicles comfort assessment through comparison with experimental measurements. Veh Syst Dyn 2002;38(3):165–83. https://doi.org/10.1076/vesd.38.3.165.8287.
[15] Xue R, Ren Z, Fan T, Rakheja S. Vertical vibration analysis of a coupled vehicle-container model of a high-speed freight EMU. Veh Syst Dyn 2020. https://doi.org/10.1080/00423114.2020.1850810.
[16] Liu X, Zhang Y, Xie S, Zhang Q, Guo H. Fatigue failure analysis of express freight sliding side covered wagon based on the rigid-flexibility model. Int J Struct Integr 2019;12:98–108. https://doi.org/10.1108/IJSI-11-2019-0122.
[17] Stichel S. The influence of underframe structural flexibility on the hunting behaviour of a freight wagon. Adv Transp 2000;7:725–36.
[18] Magalhães H, Madeira JFA, Ambrósio J, Pombo J. Railway vehicle performance optimisation using virtual homologation. Veh Syst Dyn 2016;54(9):1177–207. https://doi.org/10.1080/00423114.2016.1196821.
[19] Iwnicki SD, Stichel S, Orlova A, Hecht M. Dynamics of railway freight vehicles. Veh Syst Dyn 2015;53(7):995–1033. https://doi.org/10.1080/00423114.2015.1037773.
[20] Zhang D, Clarke DB, Peng Q, Gao H, Dong C. Effect of the combined centre of gravity on the running safety of freight wagons. Veh Syst Dyn 2019;57(9):1271–86. https://doi.org/10.1080/00423114.2018.1494841.
[21] Evans J, Berg M. Challenges in simulation of rail vehicle dynamics. Veh Syst Dyn 2009;47(8):1023–48. https://doi.org/10.1080/00423110903071674.
[22] Hoffmann M. On the dynamics of European two-axle railway freight wagons. Nonlinear Dyn 2008;52(4):301–11. https://doi.org/10.1007/s11071-007-9279-1.
[23] Hoffmann M. Dynamics of European two – axle freight wagons. Technical University of Denmark 2006.
[24] Stichel S. On freight wagon dynamics and track deterioration. Proc Inst Mech Eng Part F J Rail Rapid Transit 1999;213(4):243–54. https://doi.org/10.1243/0954409991531182.
[25] Ouyang S, Sui F. Experimental modal analysis of high-speed railway carriage. INTERNOISE 2014–43rd Int. Congr. Noise Control Eng. Improv. World Through Noise Control 2014.
[26] Bragança C, Neto J, Pinto N, Montenegro PA, Ribeiro D, Carvalho H, et al. Calibration and validation of a freight wagon dynamic model in operating conditions based on limited experimental data. Veh Syst Dyn 2021:1–27. https://doi.org/10.1080/00423114.2021.1933091.
[27] Sichani MT, Ahmadian H. Identification of Railway Car Body Model Using Operational Modal Analysis. Proc 8th Int Railw Transp Conf Tehran, Islam Repub. Iran 2006.
[28] Aravanis T-C, Sakellariou JS, Fassois SD. Spectral analysis of railway vehicle vertical vibration under normal operating conditions. Int J Rail Transp 2016;4(4): 193–207. https://doi.org/10.1080/23248378.2016.1221749.
[29] Ticona Melo LR, Ribeiro D, Calçada R, Bittencourt TN. Validation of a vertical train–track–bridge dynamic interaction model based on limited experimental data. Struct Infrastruct Eng 2020;16(1):181–201. https://doi.org/10.1080/15732479.2019.1605394.
[30] Akiyama Y, Tomioka T, Takigami T, Aida K, ichiro, Kamada T. A three-dimensional analytical model and parameter determination method of the elastic vibration of a railway vehicle carbody. Veh Syst Dyn 2020;58:545–68. https://doi.org/10.1080/00423114.2019.1590606.
[31] Sichani MT, Ahmadian H. Model updating of railway car body using operational modal testing results. Proc 2nd Int Oper Modal Anal Conf IOMAC. 2007 2007..
[32] Szafrański M. A dynamic vehicle-bridge model based on the modal identification results of an existing EN57 train and bridge spans with non-ballasted tracks. Mech Syst Signal Process 2021;146:107039. https://doi.org/10.1016/j.ymssp.2020.107039.
[33] Quike P, OBrien EJ, Bowe C, Cantero D, Malekjafarian A. The calibration challenge when inferring longitudinal track profile from the inertial response of an in-service train. Can J Civ Eng 2021:cjce-2020-0069. https://doi.org/10.1139/cjce-2020-0069.
[34] Ulayar AR, Amendoeira C, Henriques T, Lopes M, Sousa R. Train Logistics n.d. http://www.trainlogistic.com (accessed 27 February 2021).
[35] Ribeiro D, Costa B, Cruz L, Oliveira M, Alves V, Montenegro P, et al. Simulation of the Dynamic Behavior of a Centenary Metallic Bridge under Metro Traffic Actions Based on Advanced Interaction Models. Int J Struct Stab Dyn 2021;21(04): 2150057. https://doi.org/10.1142/S0219455421500577.
[36] Meixedo A, Ribeiro D, Santos J, Calçada R, Todd M. Progressive numerical model validation of a bowstring-arch railway bridge based on a structural health monitoring system. J Civ Struct Heal Monit 2021. https://doi.org/10.1007/s13349-020-00461-w.
[37] UIC Code 517 - Wagons - Suspension gear - Standardisation 2007.
[38] True H, Hoffmann M, Jönsson PA. The design and performance of the European freight wagon standard suspensions. Am. Soc. Mech. Eng. Rail Transp. Div. RTD, vol. 30, ASMEDC; 2005, p. 9–18. https://doi.org/10.1115/IMECE2005-79227.
[39] Piotrowski J. Model of the UIC link suspension for freight wagons. Arch Appl Mech (Ingenieur Arch 2003;73(7):517–32. https://doi.org/10.1007/s00419-003-0305-6.
[40] Jönsson P-A, Stichel S, Persson I. New simulation model for freight wagons with UIC link suspension. Veh Syst Dyn 2008;46(sup1):695–704. https://doi.org/10.1080/00423110802036976.
[41] ANSYS Inc. ANSYS® Academic Research Mechanical Release 18.1. 2018.
[42] Hertz HR. Ueber die Berührung fester elastischer Körper (On Contact Between Elastic Bodies). J Für Die Reine Und Angew Math (Crelle's Journal) 1882;1882. https://doi.org/10.1515/crll.1882.92.156.
[43] Gérard J, Guibal D, Paradis S, Vernay M, Beauchêne J, Brancheriau L, et al. Tropix 7 2011. https://doi.org/10.18167/74726F706978.
[44] ARTeMIS. ARTeMIS Extractor Pro - Academic License, User's Manual, SVS 2009.
[45] The MathWorks Inc. MATLAB (R2020a). Natick, Massachusetts: 2020.
[46] Ribeiro D, Calçada R, Brehm M, Zabel V. Calibration of the numerical model of a track section over a railway bridge based on dynamic tests. Structures 2021;34: 4124–41. https://doi.org/10.1016/j.istruc.2021.09.109.
[47] Jaishi B, Ren W-X. Structural Finite Element Model Updating Using Ambient Vibration Test Results. J Struct Eng 2005;131(4):617–28. https://doi.org/10.1061/(ASCE)0733-9445(2005)131:4(617).